Numerical Solution of Constrained Curvature Flow for Closed Planar Curves

Miroslav Kolář, Michal Beneš, and Daniel Ševčovič

Abstract. This paper presents results of computational studies of the evolution law for the constrained mean curvature flow. The considered motion law originates in the theory of phase transitions in crystalline materials. It describes the evolution of closed embedded curves with constant enclosed area. In the paper, the motion law is treated by the parametric method, which leads into the system of degenerate parabolic equations for the parametric description of the curve. This system is numerically solved by means of the flowing finite volume method enhanced by tangential redistribution. Qualitative and quantitative results of computational studies are presented.

1   Introduction

The objective of this article is to investigate the numerical solution of nonlocal, area preserving curvature flow for closed planar curves. The flow is given by the following geometric evolution equation

$$v_\Gamma = -\kappa_\Gamma + F, \quad \text{where } F = \frac{1}{L(\Gamma_t)} \int_{\Gamma_t} \kappa_\Gamma \mathrm{d}s, \tag{1}$$

$$\Gamma_t|_{t=0} = \Gamma_{ini}. \tag{2}$$

Here, Γ_t is a C^1 smooth Jordan curve of the length $L(\Gamma_t) = \int_{\Gamma_t} \mathrm{d}s$ evolving in time. It is evolved in the direction of the outer normal with velocity v_Γ and driven by the curvature κ_Γ and the particular non-local force term F. Our objective is to find a family $\{\Gamma_t : t \in (0, T_{max})\}$ of closed nonselfintersecting planar curves evolving from the initial curve Γ_{ini} according to (1). Although the evolution equation (1) does not involve a tangential redistribution term, any parametrization of the initial curve in (2) inherently incorporates initial redistribution of grid points which is then propagated along curve evolution.

M. Kolář · M. Beneš

Department of Mathematics, Faculty of Nuclear Sciences and Physical Engineering, Czech Technical University in Prague, Trojanova 13, 120 00, Prague 2, Czech Republic
e-mail: kolarmir@fjfi.cvut.cz; michal.benes@fjfi.cvut.cz

D. Ševčovič
Department of Applied Mathematics and Statistics, Faculty of Mathematics, Physics and Informatics, Comenius University, 842 48, Bratislava, Slovakia
e-mail: sevcovic@fmph.uniba.sk

Equation (1) belongs to a family of constrained curvature driven flows described by general evolution law

$$v_\Gamma = -\kappa_\Gamma + G,$$

where G is a possibly non-local force term preserving some quantity. In our case, the particular choice of the force term as $\int_{\Gamma_t} \kappa_\Gamma \mathrm{d}s / L(\Gamma_t)$ leads to the area preserving curvature flow. Such geometric motion laws similar to (1) are discussed in the literature (see, e.g., [1–5]). Another geometric evolution laws similar to (1) treating, e.g., the length preserving curvature flow or the isoperimetric ratio gradient flow are studied and discussed in, e.g., [6].

The constrained motion driven by the curvature has also been investigated, in [7,8] within the context of a modification of the Allen-Cahn equation (see [9,10]). The non-local character of the geometric governing equation (1) is strongly connected with the studies of the recrystallization phenomena, where a fixed, previously melted volume of the liquid phase solidifies again (see [11]).

2   Parametric Method

The method presented in this paper is based on parametric description of the smooth time-dependent curve Γ_t ($t \geq 0$) by means of the vectorial mapping $\mathbf{X}(u,t) = (X_1(u,t), X_2(u,t))$, where $u \in [0,1]$ is a dimensionless parameter in a given fixed interval. Throughout this paper, the parametrization is orientated counter-clockwise and periodic boundary conditions at $u = 0$ and $u = 1$ are imposed, i.e., $\mathbf{X}(0,t) = \mathbf{X}(1,t)$ and $\partial_u \mathbf{X}(0,t) = \partial_u \mathbf{X}(1,t)$.

Consequently, geometrical quantities of interest can be prescribed by the parametrization $\mathbf{X}$. The unit tangent and normal vectors $\mathbf{t}_\Gamma$ and $\mathbf{n}_\Gamma$ are defined straightforwardly, and the curvature is given by Frenet formulae:

$$\mathbf{t}_\Gamma = \frac{\partial_u \mathbf{X}}{|\partial_u \mathbf{X}|}, \quad \mathbf{n}_\Gamma = \frac{\partial_u \mathbf{X}^\perp}{|\partial_u \mathbf{X}|}, \quad \kappa_\Gamma(\mathbf{X}) = -\frac{1}{|\partial_u \mathbf{X}|} \partial_u \left(\frac{\partial_u \mathbf{X}}{|\partial_u \mathbf{X}|} \right) \cdot \mathbf{n}_\Gamma.$$

Here $\mathbf{X}^\perp = (X_2, -X_1)$. This choice is in accordance with the rule $\det(\mathbf{n}_\Gamma, \mathbf{t}_\Gamma) = 1$. Notice that in our case the curvature of the unit circle is $\kappa_\Gamma = 1$. The normal velocity is just a projection of the point velocity $\mathbf{v}_\Gamma = \partial_t \mathbf{X}$ to the normal direction $\mathbf{n}_\Gamma$, i.e., $v_\Gamma = \mathbf{v}_\Gamma \cdot \mathbf{n}_\Gamma$. Finally, the curve Γ_t evolves according to the law (1) provided the parametric mapping $\mathbf{X}$ satisfies the following system of degenerate parabolic equations

$$\partial_t \mathbf{X} = \frac{1}{|\partial_u \mathbf{X}|} \partial_u \left(\frac{\partial_u \mathbf{X}}{|\partial_u \mathbf{X}|} \right) + F \frac{\partial_u \mathbf{X}^\perp}{|\partial_u \mathbf{X}|}, \tag{3}$$

$$\mathbf{X}|_{t=0} = \mathbf{X}_{\mathrm{ini}}, \tag{4}$$

for $t \in (0, T_{max})$ and $u \in [0,1]$. The driving force F of flow (1) written by means of the parametrization $\mathbf{X}$ becomes

$$F = \int_{\Gamma_t} \kappa_\Gamma \mathrm{d}s / L(\Gamma_t) = \int_0^1 \kappa_\Gamma(\mathbf{X}) |\partial_u \mathbf{X}| \mathrm{d}u / \int_0^1 |\partial_u \mathbf{X}| \mathrm{d}u.$$

For details on this approach, we refer he reader to, e.g., [12–15]. Another approach dealing with area preserving flows is based on the tangential velocity dependent on the Laplace-Beltrami operator acting on the curvature. For such geometric flows (see [16]) is well known that they describe area preserving geometric flows. The main advantage of this approach is in fast and straightforward numerical treatment, which is noticeable especially when comparing to other interface capturing methods, such as the level-set method [17] or the phase-field method [18]. However, this approach itself is not able to treat the cases, where changes in curve topology occurs (like merging or splitting). For such a task, separate algorithms have to be developed [19].

We denote

$$A(\Gamma_t) = \frac{1}{2} \int_0^1 \det(\mathbf{X}, \partial_u \mathbf{X}) \mathrm{d}u. \tag{5}$$

Then the flow (1) preserves the quantity $A = A(\Gamma_t)$, i.e., $A(\Gamma_t) = A(\Gamma_{ini})$ for all $t \geq 0$. For a closed curve, the quantity $A(\Gamma_t)$ represents the enclosed area. Here we remind the following result, which is known for the case when Γ_t is the Jordan curve (see e.g., [20]).

Remark 1. Let $\{\Gamma_t\}_{t \geq 0}$ be a family of C^1 smooth Jordan curves evolving in the normal direction according to (1) and parametrized by the mapping $\mathbf{X}$ satisfying $(3 - 4)$. Then

$$\frac{\mathrm{d}A(\Gamma_t)}{\mathrm{d}t} = 0.$$

3   Tangential Effects

By nature of law (1), the tangential terms do not affect the shape of the curve. Hence they are not important from the analytical point of view. However, considering numerical treatment of (1), properly chosen tangential terms can significantly affect the solution. Discussion on the concept of the so called tangential redistribution can be found in, e.g., [21]. For technical details of the tangential redistribution for our parametric model, we refer the reader to [6,12]. Notice that these papers are concerned with non-locally dependent tangential velocities. As far as locally dependent tangential velocities are concerned, we mention a tangential velocity proposed and analyzed by Dziuk and Deckelnick in [22]. Resulting parametric model (3) enhanced by tangential redistribution has the following form

$$\partial_t \mathbf{X} = \frac{1}{|\partial_u \mathbf{X}|} \partial_u \left(\frac{\partial_u \mathbf{X}}{|\partial_u \mathbf{X}|} \right) + \alpha \frac{\partial_u \mathbf{X}}{|\partial_u \mathbf{X}|} + F \frac{\partial_u \mathbf{X}^\perp}{|\partial_u \mathbf{X}|}, \tag{6}$$

where α is a possibly non-local function of time and curvature. In our model, we use the tangential redistribution discussed and applied in [6], which forces the discretization points to be placed asymptotically uniformly along the curve. In this case, the tangential term α satisfies

$$\frac{1}{|\partial_u \mathbf{X}|}\partial_u \alpha = \kappa_\Gamma v_\Gamma - \frac{1}{L(\Gamma_t)}\int_{\Gamma_t} \kappa_\Gamma v_\Gamma \mathrm{d}s + \omega\left(\frac{L(\Gamma_t)}{|\partial_u \mathbf{X}|} - 1\right),$$

where ω is a given scalar parameter. To ensure the uniqueness of the solution, α is required to fulfill the condition $\int_{\Gamma_t} \alpha \mathrm{d}s / L(\Gamma_t) = 0$.

4   Numerical Solution

In our approach, the time evolving curve Γ_t is approximated as a piece-wise linear curve, and for the spatial discretization of governing equations (6), the flowing finite volume method is used. For technical details and discussion on the method, we refer the reader to, e.g., [5,6,12,13,21]. The discrete nodes $\mathbf{X}_i = \mathbf{X}(t, u_i)$ for $i = 0, \ldots M$ are placed along the curve Γ_t, and linear segments connecting the neighboring nodes represent the finite volumes. We denote $d_j = |\mathbf{X}_j - \mathbf{X}_{j-1}|$ for $j = 1, \ldots M$, where $\mathbf{X}_0 = \mathbf{X}_M$. Similarly to the discrete nodes $\mathbf{X}_i$, we consider discretized tangential coefficients α_i. For the way how to appropriately calculate the redistribution coefficients α_i within the context of used numerical scheme see, e.g., [12], where the problem of tangential redistribution is analyzed in detail. Finally, our semi-discrete scheme for solving (6) within the context of the motion law (1) is the following

$$\frac{d\mathbf{X}_i}{dt}\frac{d_i + d_{i+1}}{2} = \left(\frac{\mathbf{X}_{i+1} - \mathbf{X}_i}{d_{i+1}} - \frac{\mathbf{X}_i - \mathbf{X}_{i-1}}{d_i}\right) + F\frac{(\mathbf{X}_{i+1}^\perp - \mathbf{X}_{i-1}^\perp)}{2}$$
$$+\alpha_i\frac{(\mathbf{X}_{i+1} - \mathbf{X}_{i-1})}{2}, \tag{7}$$

$$\kappa_i = -\frac{2}{d_i + d_{i+1}}\left(\frac{\mathbf{X}_{i+1} - \mathbf{X}_i}{d_{i+1}} - \frac{\mathbf{X}_i - \mathbf{X}_{i-1}}{d_i}\right)\cdot\frac{\mathbf{X}_{i+1}^\perp - \mathbf{X}_{i-1}^\perp}{d_i + d_{i+1}} \tag{8}$$

$$F = \frac{1}{\sum_{l=1}^M d_l}\sum_{l=1}^M \kappa_l\frac{d_{l+1} + d_l}{2}, \tag{9}$$

$$\mathbf{X}_i(0) = \mathbf{X}_{ini}(u_i), \tag{10}$$

for $i = 1, \ldots, M$. This system is solved by means of the 4th-order explicit Runge-Kutta-Merson scheme with the automatic time step (denoted as Δt_k) control and the tolerance parameter $\varepsilon = 10^{-6}$. The initial time step was chosen as h^2, where $h = 1/M$ is the mesh size dividing the parameter range $[0, 1]$.

5   Computational Studies

We present some results of our qualitative and quantitative computational studies for the closed curves dynamics driven by (6) and treated by numerical scheme (7 – 10). In the following examples, we demonstrate how a solution of (6) evolves in time and approaches the circular shape.

We have measured the experimental orders of convergence (EOC) for our scheme. The measurements were performed indirectly – as the testing parameter for computation of EOC, the quantity $A(\Gamma_t)$ representing the area of the enclosed curve was chosen. We measured the differences given by the area at the initial time $A(\Gamma_{ini})$, and the areas $A(\Gamma_{T_i})$ at given data output times $T_i, i = 1, \ldots, N$. For given mesh with M segments, we evaluate the maximum and the discrete L_1 (with time steps Δt_k) norms, i.e.,

$$error_1(M) = \max_{i=1,2,\ldots N} |A(\Gamma_{ini}) - A(T_i)|,$$

$$error_2(M) = \frac{1}{T_N} \sum_{k=1}^{N} |A(\Gamma_{ini}) - A(T_i)| \Delta t_k.$$

Both errors depend on the number of finite volumes M. We estimate the order of convergence between two meshes with M_1 and M_2 volumes as

$$EOC = \log\left(error_i(M_1)/error_i(M_2)\right)/\log\left(M_2/M_1\right), i = 1, 2.$$

Example 1. In Figure 1, we show the qualitative behavior of the numerical solution of problem (1), where the initial eight-folded curve Γ_{ini} is given as $\mathbf{X}(0, u) = r_{ini}(u)(\cos 2\pi u, \sin 2\pi u), u \in [0, 1]$ with r_{ini} defined as

$$r_{ini}(u) = 0.5 + 0.2 \cos(16\pi u), \qquad u \in [0, 1].$$

The motion is captured in the time interval $[0, 0.5]$ and the number of finite volumes in Figure 1 is $M = 200$. The curve Γ_t approaches the circular shape and the quantity $A(\Gamma_t)$ – the area enclosed by the curve Γ_t is preserved. The initial curve Γ_{ini} encloses the area of 0.84823 and at $t = 0.5$ the curve Γ_t encloses the area of 0.846215385275. The values of EOC for various meshes are in Table 1.

Table 1. Table of EOCs for Example 1

M	$error_1$	EOC	$error_2$	EOC
100	0.007069986241	–	0.007061259667	–
200	0.002014614725	1.8112	0.002015348016	1.8089
300	0.000944083352	1.8694	0.000945069453	1.8677
400	0.000543526916	1.9192	0.000544287109	1.9180
500	0.000352173540	1.9447	0.000352741175	1.9439

Example 2. In Figure 2, we show the qualitative behavior of the numerical solution of problem (1), where the initial curve Γ_t with high variation of
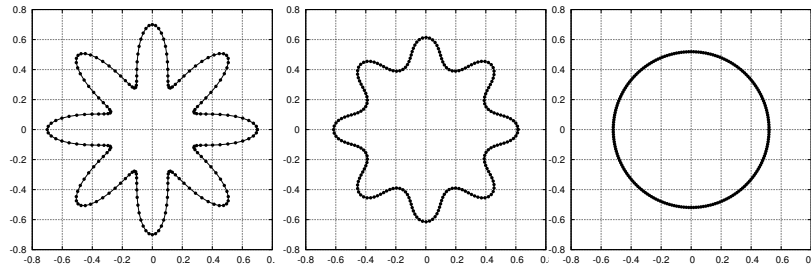
Fig. 1. The area-preserving mean curvature flow (1) in Example 1, where the initial 8-folded curve asymptotically approaches the circular shape. The curve Γ_t is depicted for time levels $t = 0$, $t = 0.005$, and $t = 0.5$.

curvature is given by the parametric equations

$$\mathbf{X}(0, u) = \big((1 + 0.4\cos(12\pi u) + 0.2\cos(6\pi u))\cos(2\pi u),$$
$$(2.5 + 0.4\sin(12\pi u) + 0.2\sin(4\pi u))\sin(2\pi u)\big) \qquad u \in [0, 1].$$

The motion is captured in the time interval $[0, 5]$ and the number of finite volumes in Figure 2 is $M = 200$. The curve Γ_t approaches the circular shape and the quantity $A(\Gamma_t)$ – the area enclosed by the curve Γ_t is preserved. The initial curve Γ_{ini} encloses the area of 7.85398 and at $t = 5$ the curve Γ_t encloses the area of 7.863369794295. The values of EOC for various meshes are in Table 2.
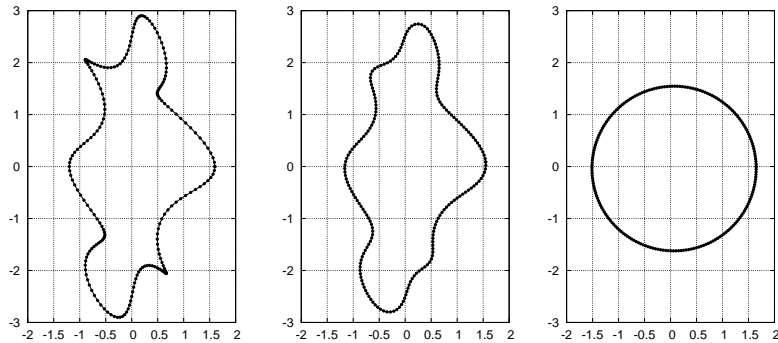
Fig. 2. The area-preserving mean curvature flow (1) in Example 2, where the initial curve asymptotically approaches the circular shape. The curve Γ_t is depicted for time levels $t = 0$, $t = 0.025$, and $t = 5$.

Table 2. Table of EOCs for Example 2

M	$error_1$	EOC	$error_2$	EOC
100	0.030290732384	–	0.029986248027	–
200	0.009389794295	1.6897	0.009293578786	1.6900
300	0.004615850440	1.7514	0.004570165389	1.7505
400	0.002751185152	1.7987	0.002724720989	1.7978
500	0.001827489090	1.8333	0.001810281006	1.8324

6   Conclusion

In this paper, we investigated the area-preserving mean curvature flow for closed Jordan curves in terms of qualitative and quantitative behavior of the approximate solution obtained numerically by means of the flowing finite volume method enhanced by the tangential redistribution of discretization points. Computational results suggest that the order of convergence of our numerical scheme approaches 2 in space when the convergence ratio is measured for the error measured in the enclosed area. Our studies are in agreement with theoretical indications that the solution of constrained problem (1) approaches the circular shape in steady state (see [1,7]). This behavior corresponds to real expectations in modeling of recrystallization phenomena in solids.

Acknowledgement

References

1. M. Gage, *On an area-preserving evolution equation for plane curves*, Contemp. Math **51** (1986), 51–62.

2. I. C. Dolcetta, S. F. Vita and R. March, *Area preserving curve shortening flows: from phase separation to image processing*, Interfaces and Free Boundaries **4** (2002), 325–343.

3. C. Kublik, S. Esedoḡlu and J. A. Fessler, *Algorithms for Area Preserving Flows*, SIAM Journal on Scientific Computing **33** (2011), 2382–2401.

4. J. McCoy, *The surface area preserving mean curvature flow*, Asian J. Math. **7** (2003), 7–30.

5. M. Kolář, M. Beneš and D. Ševčovič, *Computational studies of conserved mean-curvature flow*, Mathematica Bohemica **139**:4 (2014), 677–684.

6. D. Ševčovič and S. Yazaki, *On a gradient flow of plane curves minimizing the anisoperimetric ratio*, IAENG International Journal of Applied Mathematics **43** (2013), 160–171.

7. J. Rubinstein and P. Sternberg, *Nonlocal reaction-diffusion equations and nucleation*, IMA Journal of Applied Mathematics **48** (1992), 249–264.

8. M. Beneš, S. Yazaki and M. Kimura, *Computational studies of non-local anisotropic Allen-Cahn equation*, Mathematica Bohemica **134**:4 (2011), 429–437.

9. J. W. Cahn and J. E. Hilliard, *Free energy of a nonuniform system III. Nucleation of a two-component incompressible uid*, Journal of Chemical Physics **31** (1959), 688–699.

10. S. Allen and J. Cahn, *A microscopic theory for antiphase boundary motion and its application to antiphase domain coarsening*, Acta Metallurgica **27** (1979), 1084–1095.

11. I. V. Markov, *Crystal Growth for Beginners: Fundamentals of Nucleation, Crystal Growth, and Epitaxy, 2 ed.*, World Scientific Publishing Company (2004).

12. M. Kolář, M. Beneš, D. Ševčovič and J. Kratochvíl, *Mathematical Model and Computational Studies of Discrete Dislocation Dynamics*, IAENG International Journal of Applied Mathematics **45**:3 (2015), 198–207.

13. V. Minárik, M. Beneš, J. Kratochvíl, *Simulation of dynamical interaction between dislocations and dipolar loops*, Journal of Applied Physics **107** (2010), 061802.

14. K. Deckelnick, *Parametric mean curvature evolution with a dirichlet boundary condition*, Journal für die reine und angewandte Mathematik **459** (1995), 37–60.

15. K. Deckelnick, G.Dziuk, C.M. Elliott, *Computation of geometric partial differential equations and mean curvature flow*, Acta Numerica **14** (2005), 139–232.

16. J.W. Barrett, H. Garcke, and R. Nürnberg, *On the variational approximation of combined second and fourth order geometric evolution equations*, SIAM Journal on Scientific Computing **29**:3 (2007), 1006–1041.

17. S. Osher, J. Sethian, *Fronts propagating with curvature dependent speed: Algorithms based on Hamilton-Jacobi formulations*, Journal of Computational Physics **79** (1988), 12–49.

18. M. Beneš, *Diffuse-interface treatment of the anisotropic mean-curvature flow*, Applications of Mathematics **48**:6 (2003), 437–453.

19. P. Pauš, J. Kratochvíl and M. Beneš, *A dislocation dynamics analysis of the critical cross-slip annihilation distance and the cyclic saturation stress in fcc single crystals at different temperatures*, Acta Materialia **61** (2013), 7917–7923.

20. D. Ševčovič and K. Mikula, *Evolution of plane curves driven by a nonlinear function of curvature and anisotropy*, SIAM Journal on Applied Mathematics **61**:3 (2001), 1473–1501.

21. K. Mikula and D. Ševčovič , *Computational and qualitative aspects of evolution of curves driven by curvature and external force*, Computing and Visualization in Science **6**:3 (2004), 211–225.

22. K. Deckelnick and G. Dziuk, *On the approximation of the curve shortening flow*, Pitman Research Notes in Mathematics Series **326** (1995), 100–108.